A&A 389, 802–811 (2002)
DOI: 10.1051/0004-6361:20020658

Astronomy & Astrophysics

Compton reflection and iron fluorescence in BeppoSAX observations of Seyfert type 1 galaxies

G. C. Perola[1], G. Matt[1], M. Cappi[2], F. Fiore[3], M. Guainazzi[4], L. Maraschi[5], P. O. Petrucci[5,6], and L. Piro[7]

[1] Dipartimento di Fisica, Università degli Studi "Roma Tre", Via della Vasca Navale 84, 00146 Roma, Italy
[2] Istituto di Astrofisica Spaziale e Fisica Cosmica, CNR, Via Gobetti 101, 40129 Bologna, Italy
[3] Osservatorio Astronomico di Roma, Via dell'Osservatorio, 00044 Monteporzio Catone, Italy
[4] XMM-Newton SOC, VILSPA–ESA, Apartado 50727, 28080 Madrid, Spain
[5] Osservatorio Astronomico di Brera, Via Brera 28, 20121 Milano, Italy
[6] Laboratoire d'Astrophysique de l'Observatoire de Grenoble, BP 53X, 38041 Grenoble Cedex, France
[7] Istituto di Astrofisica Spaziale e Fisica Cosmica, CNR, Via Fosso del Cavaliere, 00133 Roma, Italy

Received 18 September 2001 / Accepted 25 April 2002

Abstract. A sample of nine bright Seyfert 1 and NELG type galaxies, observed with BeppoSAX, is analyzed to assess on a truly broad band basis (0.1–200 keV) the issue of the spectral contributions of Compton reflection and iron line fluorescence from circumnuclear gas. The empirical description adopted for the direct continuum is the commonly used power law with an exponential cut–off. The most direct test of the theoretical predictions, namely that the equivalent width of the line, W_α, and the strength R of the reflection relative to the direct continuum are closely related to each other, gives a substantially positive result, that is their mean ratio is very close to expectation, and only a modest spread in the iron abundance seems implied. The existence of a steep correlation between R and the slope Γ of the power law is not confirmed. A weak evidence is found that the existence of a very shallow trend to increase on average with Γ cannot be altogether excluded in both R and W_α, but needs to be tested with a larger sample. The energy E_f in the exponential cut–off spans a range from about 80 to more than 300 keV. A possible correlation is found, with E_f increasing on average with Γ: if ignored, for instance by keeping E_f at a fixed value in a sample study, it could be cause of artificial steepening in a correlation between R and Γ.

Key words. galaxies: Seyfert – X-rays: galaxies

1. Introduction

Observations with the *Ginga* satellite in the 2–18 keV band of a sample of bright Active Galactic Nuclei (Nandra & Pounds 1994), following the discoveries with the same satellite by Piro et al. (1990), Matsuoka et al. (1990) and Pounds et al. (1990), definitely confirmed the presence of reprocessed, in addition to the direct, power law emission, as predicted by e.g. Guilbert & Rees (1988), Lightman & White (1988), George & Fabian (1991), Matt et al. (1991). The reprocessed radiation consists of two main components. The first is seen as a broad excess rising above about 10 keV, due to Compton reflection of the power law by optically thick, low ionization matter, the second is K_α fluorescence of mainly "cold" iron at 6.4 keV. Both appear to be common features in Seyfert galaxies of type 1 and intermediate between type 1 and 2 (objects of the latter type are often referred to as Narrow Emission Line Galaxies, NELG, their X-ray spectra are typically affected by a substantial, order 10^{22-23} H atoms cm^{-2}, neutral absorbing column).

Once the inclination angle i between line of sight and material is adopted, the amplitude of the reflection relative to the power law can be converted into a measure $R = \Omega/2\pi$ of the solid angle subtended by the reflector. Through a reanalysis of *Ginga* data for 23 radio–quiet Seyfert 1 and NELG, Zdziarski et al. (1999) found evidence of a strong correlation between R (estimated for a fiducial value of $i = 30°$) and the photon slope Γ of the power law, which they tentatively describe with a function where the average $R \propto \Gamma^v$, v about 12: R rises from about 0.1 at $\Gamma = 1.7$ to about 1 at $\Gamma = 2.1$. They argue that the correlation is not an orientation effect, and, in the framework of the models where the production of the power law is associated with a very hot medium that comptonizes soft photons, they tentatively attribute it to a feedback of the additional photons from the reflection on the physical state of that medium. At present, however,

Send offprint requests to: G. C. Perola,
e-mail: perola@fis.uniroma3.it

its real significance, at least in its quantitative terms, is in doubt, because the existence of a strong correlation between these two variables in the fit of single observations is likely to bias substantially the result. Vaughan & Edelson (2001), for instance, on the basis of extensive simulations of data obtained with the PCA instrument onboard the RossiXTE satellite in an energy band similar to that of the *Ginga* data, have shown that a spurious correlation can be produced. Done & Nayakshin (2001) proposed yet an alternative possibility, namely that the correlation could be an artifact of the single–zone ionization (neutral in practice) model adopted for the reflector: however the simulations of *Ginga* spectra with their sophisticated model show that the correlation should be much shallower than the analytical description quoted above.

The equivalent width W_α of the iron fluorescence line, which inevitably arises in the reflecting material, is expected to be proportional to R. However, a line with W_α up to about 100 eV, that is a substantial fraction of the observed values, in an optimal geometrical arrangement can be produced also by marginally thin gas (e.g. Woźniak et al. 1998). Thanks to the superior energy resolution, the observations with the ASCA satellite of a representative sample of objects (Nandra et al. 1997) have shown that in most cases the line is resolved and broader than the velocity spread of the optical Broad Line Region (BLR). Moreover the first ASCA observation of MCG–6-30-15 (Tanaka et al. 1995) revealed a profile consistent with the special and general relativistic effects predicted for a line originating in the innermost regions of a flat accretion disk (Fabian et al. 1989). Although the line width in this object turned out to be rather extreme compared to the others in the Nandra et al. (1997) sample, it is widely believed (e.g. Fabian et al. 2000) that the fluorescent gas is most likely associated with the optically thick accretion disk, and therefore the broad line W_α should correlate with R. Unfortunately the ASCA band, being restricted to less than 10 keV, is inadequate to estimate R, and because of the variability which typically affects the continuum emission of these objects (in addition to reported cases of variations in the line, e.g. Weaver et al. 2001 and references in Fabian et al. 2000), the comparison of W_α, as measured with ASCA, and of R as measured with *Ginga*, would lack significance. An alternative approach chosen by Lubiński & Zdziarski (2001) aims at looking for a correlation between the broad line W_α and Γ in ASCA observations of 25 objects, which should correspond to the one between R and Γ. Their Fig. 1 shows indeed a trend, on average, in W_α (single Gaussian fit) to increase with Γ. This trend is quantified by fitting a relativistic diskline profile and an additional narrow Gaussian profile to three average spectra, each one grouped according to the slope: the hardest group ($\Gamma_{\rm av} = 1.62$) has broad $W_\alpha = 72^{+17}_{-18}$ eV, the softest group ($\Gamma_{\rm av} = 1.94$) has broad $W_\alpha = 124 \pm 26$, with an average inclination angle (a product of the diskline fit) practically the same for the three groups, $i \sim 45°$. The additional Gaussian has an average narrow W_α of about 50 eV in all three groups. The authors interpret this component as originating in marginally thin gas: this is a possibility, as mentioned above, but the alternative one that it might instead be associated with highly reflecting material well beyond the accretion disk looks at present at least equally viable. For instance, the case of NGC 4051 observed with BeppoSAX in a state of exceptionally low intensity of its power law (Guainazzi et al. 1998) shows that the narrow line can be accompanied by the right amount of reflection, likely associated with a thick molecular torus well beyond the accretion disk, as predicted (e.g. Ghisellini et al. 1994) in Seyfert type 1 and 2 unified models (Antonucci 1993). The results in Lubiński & Zdziarski (2001) have been recently criticized by Yaqoob et al. (2002), and should be regarded with some caution. Besides this criticism, we note that the trend in their Fig. 1, mentioned above and which is based on individual measurements of W_α and Γ, appears to be shallower than the one between R and Γ claimed by Zdziarski et al. (1999).

In this context, the goal of this paper is to provide an assessement of the observational contribution of the italian–dutch satellite BeppoSAX (Boella et al. 1997a). This satellite is characterized by: a very broad energy band, 0.1–200 keV, covered by its Narrow Field Instruments (NFI), namely the LECS (0.1–10 keV, Parmar et al. 1997), the MECS (1.8–10.5 keV, Boella et al. 1997b) and the PDS (13–200 keV, Frontera et al. 1997); the energy resolution of the imaging ones (LECS and MECS) $\Delta E/E \sim 0.08(E/6\,{\rm keV})^{-\frac{1}{2}}$, which is intermediate between that of ASCA and of *Ginga* at the iron line; the very effective control of the background in the PDS. These properties have shown their value for the estimate in several Seyfert 1 galaxies of the spectral parameters of interest for this paper, provided their flux in the 2–10 keV band is at least $(2\text{–}3)\times10^{-11}$ erg cm^{-2} s^{-1} (e.g. Guainazzi et al. 1999a; Perola et al. 1999).

Thanks to the signal detected in the PDS band, the strength of the reflection is basically measured in the fit by the excess counts in the 20–50 keV, where the broad maximum of this component is located, over the power law whose slope is constrained by the spectral counts in the LECS and MECS. Determining the slope of the power law is therefore the main issue, and the confidence beyond the purely statistical errors is related to the confidence that can be associated, object by object, to the treatment of additional spectral components, such as the cold and warm (ionized gas) absorbers and a generic soft excess. In addition, the power law itself may be affected by a high energy "break" (as first seen in NGC 4151, Jourdain et al. 1992), which we shall, as it is often done in the literature, empirically describe with an exponential factor, $\exp(-E/E_{\rm f})$. Since the relative strength of the reflection below and at its broad maximum is very sensitive to the Compton recoil in the scattering of higher energy photons, hence to $E_{\rm f}$, the ability to estimate both R and $E_{\rm f}$ thanks to the wide band and the efficient background control of the PDS (collimator used in rocking mode) is an asset of BeppoSAX. Nonetheless caution must be retained

on single observation measurements of the three parameters Γ, R and $E_{\rm f}$, because systematic errors on Γ, arising from an imperfect description of the spectrum at low energies, could be substantial compared to the purely statistical errors.

When the iron line is resolved, it might seem more appropriate to use models, both for the line and the associated reflection, which incorporates Doppler and relativistic effects. This approach would be physically more self-consistent, and in principle provide in addition the inclination i. However, as confirmed by observations with the *Chandra* and XMM-*Newton* satellites (detailed in Sect. 3 for our objects), the presence of a substantial narrow contribution is a rather common property, which is difficult to separate from the broad contribution with the BeppoSAX resolution, thus making this approach very tricky, particularly for the objects in our sample, where the line width is modest, $\sigma \leq 0.4$ keV. We have therefore chosen to follow a conservative approach, where the model adopted for the reflection component is static, and the line is described as a single Gaussian. We cared, though, to verify the outcome of adding to the model a narrow line at 6.4 keV: in general no improvement in the fit is achieved, moreover, when both a narrow and a broad component are found, their combined W_α does not differ significantly from that obtained with a single Gaussian.

Despite their BeppoSAX observations fulfilled the selection criteria given in Sect. 2, in order to limit the incidence in our sample of the systematic errors mentioned above, we prudently excluded objects with a too complex and variable absorber, like NGC 4151 (Piro et al. 2001), NGC 3516 (Costantini et al. 2000; Guainazzi et al. 2001) and NGC 2992 (Gilli et al. 2000). The observation of MCG–6-30-15 (Guainazzi et al. 1999b) confirmed the ASCA finding (Tanaka et al. 1995) of a very broad and asimmetrical iron line, and was also excluded because it could not be treated homogeneously with the rest of the sample.

The paper is organized in the following manner. Section 2 describes the sample of the observations used. Section 3 describes the spectral fitting procedures and the results. Section 4 illustrates the distribution of the parameters in connection with the reprocessing. Section 5 is devoted to discussion and conclusions.

2. The sample data

The sample contains observations of objects with flux in the 2–10 keV band greater than 3×10^{-11} erg cm^{-2} s^{-1}, duration longer than 50 000 s in the MECS. For some objects, with separate observations shorter than 50 000 s, after verifying with a hardness ratio analysis, as well as independent fits, that no spectral changes had occurred of such entity as to impair the reliability of the outcome relevant to the present paper, we merged two (NGC 5506, Mrk 509) or three observations (IC 4329A(2)). Several of these observations are the subject of papers already published, whose reference will be given in Sect. 3.

Table 1 lists for each object: the observation start-dates and the good exposure times in the LECS, MECS and PDS, the redshift and the galactic hydrogen column, $N_{\rm g}$, adopted, the flux in the 2–10 keV band as observed, $F_{\rm o}$, corrected for any absorption as from the model fit, $F_{\rm na}$, and its corresponding luminosity ($H_0 = 75$ km s^{-1} Mpc^{-1}).

The reduction procedure and screening criteria adopted are standard (see e.g. Guainazzi et al. 1999a). Concerning the PDS data, the Variable Rise Time (VRT) option was generally adopted, except for the observation of NGC 4593, where the Fixed Rise Time (FRT) was used. The PDS net spectra were obtained from direct subtraction of the off- from the on–source products. We verified that for none of the sample objects there was a significant contamination by hard sources in both the on- and the off–source field of view. Concerning the data from the LECS and the MECS images, the background was subtracted using spectra from blank sky files at the source position in the detectors.

The exposure times in the LECS are much shorter than in the MECS, because the former instrument is operated only during the night–time fraction of each orbit. Since the incident flux is generally recorded as variable during each observation, to take care of this inhomogeneity in the time coverage, in the fits the normalization of the LECS to the MECS was left as a free parameter. The normalization of the PDS to the MECS was instead held fixed at 0.8 (VRT selection) or 0.86 (FRT selection, Fiore et al. 1999). For the LECS data we used the version Sep. 1997 of the transfer matrix, and limited the range to 0.1–4.0 keV, where this matrix is more reliable. The energy bins chosen correspond to about one third of the instrument resolution, which itself is energy dependent.

3. Spectral analysis

The analysis of the spectral counts was performed using the software package XSPEC (Arnaud 1996, version 11.0.1). The Baseline Model Spectrum (BMS) includes: a photon power law (PL) with exponential cut–off, $AE^{-\Gamma}\exp(-E/E_{\rm f})$, together with a reflection component (RC) from a cold slab isotropically illuminated by the PL photons, subtending the solid angle $R = \Omega/2\pi$ and with inclination $\cos i$ to the line of sight (Magdziarz & Zdziarski 1995, module PEXRAV); a uniform cold absorber column at the source, $N_{\rm s}$, in addition to $N_{\rm g}$ given in Table 1; a uniform warm absorber at the source, as described in the module ABSORI, with column $N_{\rm w}$ and ionization parameter $X_{\rm i} = L_{\rm i}/nD^2$ erg cm s^{-1}, where n is the gas density and D its distance from the source of ionizing luminosity $L_{\rm i}$ in the interval 5 eV to 20 keV (for $L_{\rm i}$, assumed with a power law spectrum, we set the slope equal to Γ; the temperature of the absorbing gas was fixed as a rule at 3×10^4 K); a Gaussian line to represent the iron K$_\alpha$ fluorescence, with energy E_α, width σ_α, intensity I_α, accompanied by a Gaussian of identical width, to represent the iron K$_\beta$ (with E_β and I_β set equal to 1.1 E_α

Table 1. The sample.

Source name	Start date	LECS $T_{\rm exp}$ (s)	MECS $T_{\rm exp}$ (s)	PDS $T_{\rm exp}$ (s)	z^a	$N_{\rm g}^b$ ($\times 10^{20}$ cm-2)	$F_{\rm o}^c$ (2–10 keV)	$F_{\rm na}^c$ (2–10 keV)	$\log L_{\rm na}^d$ (2–10 keV)
MCG 8-11-11	1998-Dec.-07	29840	74865	72472	0.020	20.3^1	5.61	5.73	43.62
MCG–5-23-16	1998-Apr.-24	35825	76941	65048	0.008	8.4^2	8.73	10.00	43.06
NGC 3783	1998-Jun.-06	69135	153870	140814	0.009	9.6^2	6.44	6.86	43.00
NGC 4593	1997-Dec.-31	31426	84057	76934	0.009	2.0^1	3.72	3.79	42.74
IC 4329A (1)	1998-Jan.-02	25097	81826	75214	0.016	4.5^1	13.15	13.83	43.81
IC 4329A (2)	1998-Jul.-17 1998-Jul.-21 1998-Jul.-27	38245	106140	94772			10.68	11.18	43.71
NGC 5506	1997-Jan.-30 1998-Jan.-14	25101	77491	70842	0.006	4.3^2	7.20	9.57	42.79
NGC 5548	1997-Aug.-14	85444	312810	239320	0.017	1.6^2	3.55	3.61	43.27
Mrk 509	1998-May-18 1998-Oct.-11	41786	87834	82102	0.035	4.4^2	5.66	5.69	44.10
NGC 7469	1999-Nov.-23	99114	249780	243020	0.017	4.8^1	3.73	3.76	43.29

[a] Redshift values from Véron-Cetty & Véron (1993).
[b] Galactic H column from: (1) Elvis et al. (1989) and (2) Murphy et al. (1996).
[c] $F_{\rm o}$: Flux as observed; $F_{\rm na}$: corrected for absorption; both in units of 10^{-11} erg cm^{-2} s^{-1}.
[d] Log of luminosity corrected for absorption in erg s^{-1} ($H_0 = 75$ km s^{-1} Mpc^{-1}).

and $0.11\,I_\alpha$, George & Fabian 1991). For both reflection and absorption we adopted the element abundances in Anders & Grevesse (1993). All fits were performed with cos i fixed equal to 0.9 ($i = 26°$). Alternatively cos i was left free with R fixed equal to 1. Because the dependence on cos i of the RC shape is modest, all other parameters turned out identical in practice to those obtained with the angle fixed, and the differences in χ^2 are insignificant.

The results on the parameters of main interest for this paper are collected in Table 2. The line parameters are given in the source frame, and the line intensity I_α is also expressed as an equivalent width, W_α. The errors represent the 90% confidence interval for two parameters of interest ($\Delta\chi^2 = 4.61$, Lampton et al. 1976), a realistic choice dictated by the statistical correlation which exists between couples such as (Γ, R), (Γ, $E_{\rm f}$), (σ_α, I_α).

To be noted that in general the value of E_α is perfectly consistent with 6.4 keV, the value for "cold" iron (in agreement with previous findings, e.g. Nandra & Pounds 1994; Nandra et al. 1997; Lubiński & Zdziarski 2001). In two objects (NGC 5506 and Mrk 509) the (per se marginal) evidence of a larger value finds explanation in recent XMM-*Newton* results, reported below.

Next we briefly describe the case of each source, including the best fit values of the other BMS parameters and additional spectral components adopted to improve the quality of the fit when the BMS gave an unacceptable χ^2. Generally $X_{\rm i}$ is very poorly constrained, hence we give only its best fit value. Reference is also given to some recent results on the iron line.

MCG 8-11-11. This observation was published by Perola et al. (2000), to which we refer for the choice of neglecting in the fit the LECS counts below 0.4 keV. $N_{\rm s}$ is negligible compared to $N_{\rm g}$, the warm absorber has $N_{\rm w} = (6^{+9}_{-6}) \times 10^{20}$ cm^{-2} with $X_{\rm i} \sim 7$ erg cm s^{-1}. The iron line is not resolved, the upper limit on its width is comparable to that of the lines resolved in our sample.

MCG–5-23-16. The cold absorber in this NELG is substantial, $N_{\rm s} = (1.6 \pm 0.9) \times 10^{22}$ cm^{-2}; no signature is detected of a warm absorber. In ASCA (Weaver et al. 1997) and RossiXTE (Weaver et al. 1998) observations (comparable in flux to this one) a strong ($W_\alpha \sim$ 250 eV) and broad iron line was consistently found. In the BeppoSAX observation the line is much narrower than $\sigma_\alpha \sim 0.4$ keV, the value obtained from a single Gaussian description in both the ASCA and the RossiXTE data sets (Weaver et al. 1998); the line intensity is about twice that of the narrow Gaussian, but about one third of the sum of the narrow and broad Gaussians, as measured by Weaver et al. (1997) in their fit to the ASCA data. While this is probably yet another case of variations in the iron line (see also Smith & Done 1996 for a formally significant difference in W_α between two *Ginga* observations made a few days apart), we note that, contrary to expectation, the amount of reflection measured with RossiXTE (for a choice of $E_{\rm f} = 200$ keV, the closest to our best fit value

Table 2. Results of the spectral analysis.

Source name	Γ	$E_{\rm f}$ (keV)	R ($\cos i = 0.9$)	E_α (keV)	σ_α (keV)	I^a_α	W_α (eV)	χ^2/d.o.f.	$\cos i$ ($R = 1$)	χ^2/d.o.f.
MCG 8-11-11	$1.85^{+0.09}_{-0.05}$	166^{+215}_{-74}	$1.09^{+0.80}_{-0.39}$	6.49 ± 0.14	<0.37	$6.9^{+3.7}_{-2.4}$	117^{+63}_{-40}	132.3/141	$0.96^{+0.04}_{-0.49}$	132.6/141
MCG–5-23-16	1.81 ± 0.05	147^{+70}_{-40}	$0.66^{+0.25}_{-0.20}$	6.43 ± 0.10	<0.28	$10.0^{+3.9}_{-3.0}$	96^{+37}_{-28}	139.5/135	$0.51^{+0.24}_{-0.17}$	140.7/135
NGC 3783	1.77 ± 0.04	156^{+37}_{-40}	$0.63^{+0.20}_{-0.17}$	6.38 ± 0.09	$0.27^{+0.15}_{-0.13}$	$11.7^{+2.8}_{-2.7}$	161^{+39}_{-37}	150.4/148	$0.46^{+0.19}_{-0.14}$	148.0/148
NGC 4593	$1.94^{+0.06}_{-0.05}$	>222	$1.26^{+0.65}_{-0.40}$	6.41 ± 0.16	$0.34^{+0.36}_{-0.21}$	$9.1^{+4.4}_{-2.8}$	231^{+111}_{-72}	148.2/146	>0.63	149.0/146
IC 4329A (1)	1.89 ± 0.04	325^{+277}_{-105}	$0.63^{+0.17}_{-0.14}$	6.43 ± 0.17	$0.30^{+0.30}_{-0.26}$	$14.5^{+5.7}_{-5.6}$	104^{+41}_{-40}	146.9/141	$0.49^{+0.14}_{-0.12}$	148.2/141
IC 4329A (2)	1.90 ± 0.05	262^{+204}_{-84}	$0.73^{+0.22}_{-0.18}$	6.54 ± 0.14	$0.31^{+0.25}_{-0.15}$	$13.5^{+5.1}_{-4.0}$	123^{+46}_{-36}	154.4/140	$0.58^{+0.19}_{-0.14}$	153.9/140
NGC 5506	$2.02^{+0.09}_{-0.08}$	>298	$1.20^{+0.45}_{-0.35}$	$6.52^{+0.10}_{-0.09}$	$0.21^{+0.15}_{-0.10}$	$14.2^{+4.2}_{-3.2}$	152^{+45}_{-34}	85.3/82	>0.75	85.9/82
NGC 5548	$1.62^{+0.04}_{-0.05}$	147^{+64}_{-33}	$0.54^{+0.20}_{-0.13}$	6.41 ± 0.07	<0.13	$4.3^{+1.1}_{-0.9}$	106^{+26}_{-23}	175.1/148	$0.37^{+0.21}_{-0.12}$	176.7/148
Mrk 509	$1.58^{+0.09}_{-0.08}$	67^{+30}_{-20}	$0.58^{+0.39}_{-0.30}$	$6.64^{+0.34}_{-0.24}$	<0.87	$5.5^{+4.5}_{-2.8}$	93^{+76}_{-46}	135.7/132	$0.45^{+0.50}_{-0.33}$	137.3/132
NGC 7469	$1.88^{+0.05}_{-0.07}$	164^{+196}_{-65}	$0.50^{+0.29}_{-0.25}$	$6.44^{+0.12}_{-0.11}$	<0.47	$5.2^{+1.9}_{-1.7}$	139^{+51}_{-44}	168.4/148	$0.35^{+0.31}_{-0.20}$	168.0/148

[a] Line intensity in units of 10^{-5} photons cm^{-2} s^{-1}.

of the three adopted; Γ is identical to our best fit value; Weaver et al. 1998) is definitely not larger than in the BeppoSAX observation. Finally we note that a *Chandra* HETGS observation, briefly described in Weaver (2001), shows a narrow (*FWHM* less than 3000 Km s^{-1}) line with $W_\alpha \sim 90$ eV, similar to our value.

NGC 3783. The BMS fit is poor ($\chi^2 = 208/150$), with an excess in the residuals at low energies. With the addition of a line the χ^2 reduces to 160/147, with $E_{\rm l} = 0.59$ keV and $W_{\rm l} = 140$ eV: its strength is however almost ten times larger than that of the OVII emission lines detected by Kaspi et al. (2001) in a *Chandra* HETGS observation (when the source was fainter by only about 15%). A formally better improvement is achieved if, instead of a line, a black body is added, provided the temperature of the warm absorber is set equal to 10^5 K: the parameters given in Table 2 refer to this fit. $N_{\rm s}$ is negligible compared to $N_{\rm g}$, $N_{\rm w} = (9.6^{+3.2}_{-1.4}) \times 10^{21}$ cm^{-2}, with $X_{\rm i} \sim 15$ erg cm s^{-1}, the black body $kT = 0.18^{+0.02}_{-0.03}$ keV. The iron line is definitely resolved. The *Chandra* HETGS observation (Kaspi et al. 2001) has revealed a narrow line at 6.4 keV, with an upper limit on the width (σ less than 0.030 keV) that places its origin beyond the BLR: its intensity of $(6.6 \pm 2.1) \times 10^{-5}$ cm^{-2} s^{-1} is about 55% of that measured by us. If we include in the fit a narrow, in addition to the broad line, no improvement is attained in χ^2 and the intensity of the narrow component is not well constrained, such that a value identical to that from the *Chandra* observation is acceptable. In a recent publication (De Rosa et al. 2002) on this BeppoSAX observation, the same model adopted by us (their Model E) yields somewhat different values, in particular $\Gamma = 1.86 \pm 0.03$, $R = 0.71^{+0.20}_{-0.28}$, $W_\alpha = 210 \pm 45$, together with $N_{\rm w}$ about twice larger. The discrepancy is due to the different code adopted to describe the warm absorber, and it is not such as to influence the conclusions of the analysis following in Sect. 4. We note on the other hand the good agreement in our values of Γ and $N_{\rm w}$ with those obtained by Kaspi et al. (2001) in fitting the "line free zones" of the HETGS spectral data with a power law and a warm absorber.

NGC 4593. This observation was published by Guainazzi et al. (1999a). $N_{\rm s}$ is negligible compared to $N_{\rm g}$, and $N_{\rm w} = (2.3^{+1.1}_{-0.9}) \times 10^{21}$ cm^{-2} with $X_{\rm i} \sim 9$ erg cm s^{-1}. The iron line is resolved, W_α together with R are the largest in our sample.

IC 4329A. Observation (1) was published by Perola et al. (1999). The average flux of observation (2) is 20% lower, yet there are no statistically significant differences between the two sets of parameters (the same holds for the three pointings merged, when fitted individually, despite a 25% difference between the lowest and the highest of their flux levels). The mean values of the absorbers are: $N_{\rm s} = (2.7 \pm 1.0) \times 10^{21}$ cm^{-2}, $N_{\rm w} = (2.8^{+1.2}_{-1.0}) \times 10^{21}$ cm^{-2} with $X_{\rm i} \sim 5$ erg cm s^{-1}. The iron line is resolved. Given the strength of the source (the brightest of the sample) and the correspondingly good statistics, Perola et al. (1999) attempted a fit with a narrow Gaussian plus a relativistic disk profile, and obtained marginal evidence for the existence of the narrow component. Another marginal detection of the narrow component in a simultaneous ASCA and RossiXTE observation is presented by Done et al. (2000). In a XMM-*Newton* observation with the EPIC instrument (Gondoin et al. 2001), at a flux level 25% higher than in observation (1), the narrow (σ less than 0.06 keV) line is detected, with $W_\alpha = 43 \pm 1$ eV; a broad component is seemingly absent, but unfortunately the authors do not provide an upper limit on its equivalent width. A simultaneous and relatively short (34 000 s in the MECS)

BeppoSAX observation is used, together with the EPIC data, by Gondoin et al. (2001) to estimate $\Gamma = 1.93 \pm 0.03$ and $R = 1.1 \pm 0.3$: we believe that the estimate of R is incorrect, because obtained with a PDS to MECS normalization factor equal to an improbable value of 0.7; by fitting the BeppoSAX data, as retrieved from the public archive, with this factor equal to 0.86 (for FRT selection, see Sect. 2), we obtain best fit values of $R = 0.54$ and $\Gamma = 1.91$, fully consistent with those in Table 2.

NGC 5506. The two observations here merged have an almost identical average flux level, and when fitted individually yield similar values of the spectral parameters. The BMS fit with all three instruments gives an unacceptable $\chi^2 = 180/117$, due to an excess in the residuals well below the strong photoelectric cut–off. Since the parameters of interest do not crucially depend on how this excess is modeled, we have chosen to present in Table 2 the results obtained excluding the LECS. This NELG has a substantial $N_{\rm s} = (3.7 \pm 0.2) \times 10^{22}$ cm^{-2}, and no signatures of a warm absorber. The iron line is resolved and E_α is marginally inconsistent with 6.4 keV. This line is likely a blend of the two components recently revealed in a simultaneous XMM-*Newton* (with EPIC) and BeppoSAX observation (flux level similar to ours, Matt et al. 2001), one unresolved at 6.4 keV, the other resolved (σ about 0.25 keV) at 6.75 keV, the two with comparable intensities whose sum is consistent with the one in our observation. Matt et al. (2001) present arguments, centred on the interpretation of the iron edge seen at 7.1 keV, that a substantial fraction of the RC in this object is very likely associated with the narrow line component. Evidence supporting this interpretation can be found in a spectral variability investigation conducted with RossiXTE by Lamer et al. (2000).

NGC 5548. This observation was published by Nicastro et al. (2000). They find internally evidence of a correlation between Γ and the flux (previously discovered in *Ginga* observations by Magdziarz et al. 1998, confirmed with RossiXTE observations by Chiang et al. 2000), which has some impact on the quality of our fit. In a *Chandra* LETGS observation Kaastra et al. (2002) find evidence of a very complex warm absorber, of a soft excess and of low energy emission lines. Following Kaastra & Barr (1989), who first reported a soft excess in EXOSAT observations, they model it as a "modified black body" with temperature $kT \sim 0.1$ keV. They suggest that the NVII emission line at 0.5 keV could be identified with the low energy line detected by Nicastro et al. (2000) in the BeppoSAX observation. We therefore added to the BMS a soft component, as described by the module DISKBB in XSPEC, with kT fixed at 0.1 keV, and a line with $E_{\rm l}$ fixed at 0.5 keV. The fit yields $W_{\rm l} = 76^{+61}_{-54}$ eV, compatible with the *Chandra* result. $N_{\rm s}$ turns out negligible compared to $N_{\rm g}$, while $N_{\rm w} = (2.4 \pm 0.7) \times 10^{21}$ cm^{-2} (with $X_{\rm i} \sim 14$ erg cm s^{-1}) is marginally consistent with the column density of the dominant component in the warm absorber as estimated by Kaastra et al. (2002). The iron line is unresolved and significantly narrower (less than 0.13 keV) than in any of the other sample objects. A *Chandra* HETGS observation (Yaqoob et al. 2001), with the source at a flux level about 30% lower, has revealed a narrow line at 6.4 keV with $\sigma_\alpha = 41^{+32}_{-24}$ eV, corresponding to a velocity spread consistent with an origin in the outer BLR (a substantial contribution to the line from thick matter beyond that region is not excluded). The intensity of this line matches the one measured by us. Using the same prescriptions for a relativistic disk line used by Yaqoob et al. (2001) to obtain an upper limit of 7×10^{-5} cm^{-2} s^{-1}, we find a more stringent limit of 4×10^{-5} cm^{-2} s^{-1}: this is a factor about 2 less than in earlier ASCA records of a substantially broader line, as reported in Yaqoob et al. (2001) or in Chiang et al. (2000). In a spectral variabilty study with RossiXTE, Chiang et al. (2000) found the intriguingly paradoxical (for the reprocessing paradigm) result that W_α is anticorrelated to R.

Mrk 509. The two observations and the results from their merging were published by Perola et al. (2000): in that paper it is shown that the BMS fit leaves the line width practically unconstrained (about 3 keV) and that in this respect the situation changes radically if a soft component is added in the form of a power law (preferred to a black body). This component has $\Gamma_{\rm s} = 2.5^{+0.9}_{-0.2}$ and normalization 1.1×10^{-2} cm^{-2} s^{-1} keV^{-1} at 1 keV. $N_{\rm s}$ is negligible compared to $N_{\rm g}$, and $N_{\rm w} = (4^{+8}_{-2}) \times 10^{20}$ cm^{-2} with $X_{\rm i} \sim 16$ erg cm s^{-1}. The line width is poorly constrained and the line energy is marginally inconsistent with 6.4 keV. A XMM-*Newton* observation (with EPIC, Pounds et al. 2001) has revealed the presence of a resolved cold and of a broader ionized (6.9 keV) components. The W of the former is about twice that of the latter, their sum is consistent with the value measured by us. The source, however, was almost 3 times fainter than in our observation, thus the blend must have experienced a change in intensity by a comparable factor.

NGC 7469. The BMS fit gives a marginally acceptable $\chi^2 = 191/151$, but, like in the case of Mrk 509 as illustrated in Perola et al. (2000), the line width is practically unconstrained (about 2 keV). The addition of a soft excess in the form of a power law changes the situation radically. The slope of the soft power law is $\Gamma_{\rm s} = 3.3 \pm 0.5$, its normalization 5.5×10^{-3} cm^{-2} s^{-1} keV^{-1} at 1 keV. $N_{\rm s}$ is negligible compared to $N_{\rm g}$, and $N_{\rm w} = (6.7^{+4.3}_{-3.7}) \times 10^{20}$ cm^{-2} with $X_{\rm i} \sim 0.13$ erg cm s^{-1}. The line is not resolved, the upper limit on its width is comparable to that of the lines resolved in our sample. In a spectral variabilty study with RossiXTE, Nandra et al. (2000) detected changes in the line intensity which are not correlated with the absolute normalization of the reflection component, but they themselves doubt the reliability of their estimate of the second of the two parameters. We note that George et al. (1998) did not find evidence of a soft excess in their analysis (above 0.6 keV) of a ASCA observation with a flux 25% lower than in our data: thus the additional soft component, that we suggest here to provide a better description of the continuum of this observation, should be variable. We further note that the value of Γ in Table 2 is in good

agreement with $\Gamma = 1.92 \pm 0.02$ obtained by Nandra et al. (2000) from the integrated fit of the data in the study mentioned above, with an average flux only 10% lower than in our observation.

4. An analysis of the parameters

This section is devoted to illustrate the distribution of the parameters in the sample, in relation with the reprocessing of the PL.

4.1. W_α and R

Irrespective of model details, under the hypothesis that the line emission is entirely associated with optically thick material, to a good approximation W_α should correlate linearly with the value of R obtained for an arbitrarily fixed inclination angle. Apart from the one introduced by the measurements errors, an intrinsic scatter in W_α about the correlation can be caused by a variance in the iron abundance (for differences within a factor 2 of the cosmic value, the dependence of W_α on the iron abundance is approximately linear, see Matt et al. 1997). Furthermore, for a given R, W_α may differ according to the value of Γ, because it is proportional to the ratio of the photon number above 7.1 keV responsible for the fluorescence to the photon flux density at the line energy. The plot in Fig. 1 appears scatter dominated, and because of the rather large errors on both parameters little can be said about individual deviations from the hypothetical linear trend. The Spearman rank–order (Press et al. 1992) test, which does not take the errors into account, yields a correlation coefficient which is positive, $r_\mathrm{s} = 0.43$, but with a large, 0.2, significance level for this quantity deviating from zero. Following another approach, where the error bars are also ignored, but which seems more useful in this context, we can compute for each object the ratio of the best fit value of W_α to the value expected, given the Γ of the PL and the best fit value of R for $\cos i = 0.9$. We did that by using the Γ and angular dependence of W_α given in George & Fabian (1991), rescaled to the Anders & Grevesse (1993) abundances (see Matt et al. 1997). We obtain 0.97 for the mean value, and 0.29 for the standard deviation of the sample. A similar outcome (mean value 0.88, standard deviation 0.27) obtains when we proceed instead with R fixed equal to 1 and the best fit values of $\cos i$ to estimate the expected W_α. In our sample, then, on average the observed W_α is of the right amount expected from the simultaneously measured strength of the RC relative to the PL for the cosmic value of the element abundances. The standard deviation, being inevitably affected by the large errors on both W_α and R can be considered a limit on the variance of the iron abundance in our sample.

Concerning R, we note the concentration (6 out of 9 objects) of best fit values in the interval 0.50–0.73, or the corresponding concentration of $\cos i$ (for $R = 1$) in the interval 0.35–0.58. The absence of objects with $\cos i$ less than 0.35 (inclined more than about 70°) can be understood in the frame of the Seyfert type 1 and type 2 unified models (Antonucci 1993), where the first type takes the appearence of the second at large inclinations. The paucity of objects with small, relative to intermediate inclinations could well be a statistical fluctuation, given the modest sample size, but it may reflect intrinsic differences in R, with objects where the intrinsic R is indeed substantially less than unity.

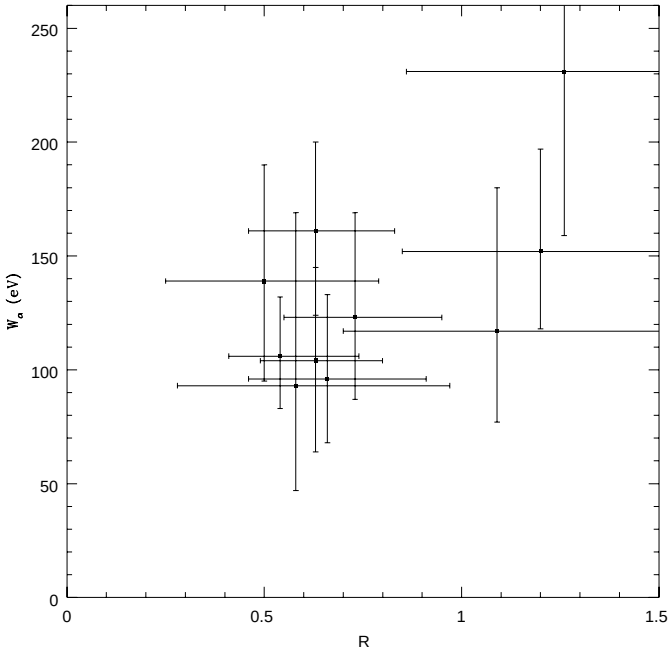

Fig. 1. W_α plotted versus R.

4.2. R and W_α versus Γ

In a diagram of R versus Γ, scatter is expected due to differences in orientation. Figure 2 shows scatter in R only above $\Gamma = 1.8$, where the largest values are confined together with values comparable to those found below. While it could be due to a statistical fluctuation in the sampling of the angles, this mere fact provides some evidence of a trend in R to increase *on average* with increasing Γ. This is reflected in the Spearman rank–order correlation coefficient r_s, which is positive and equal to 0.67, with a significance level for r_s deviating from zero equal to 0.03. The marginal significance of this evidence is further weakened by the consideration (see Sect. 1) that the two variables R and Γ remain far from independent also in the fits to our very broad band data, as can be appreciated with a simple exercise: by fitting the data of each observation with Γ fixed at the two extremes of its error bar, the values of R obtained differ typically by as much as 60 to 80% of their 90% confidence intervals. In any case, the trend in our sample (admittedly much smaller, 9 objects as opposed to 23) is definitely much shallower than the correlation found by Zdziarski et al. (1999; see also Sect. 4.3 for a supplementary cause likely to contribute to the difference).

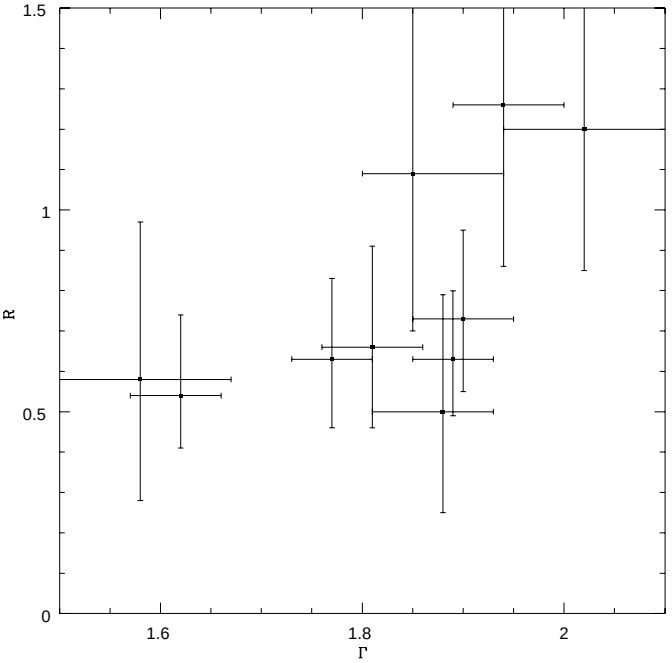

Fig. 2. R plotted versus Γ.

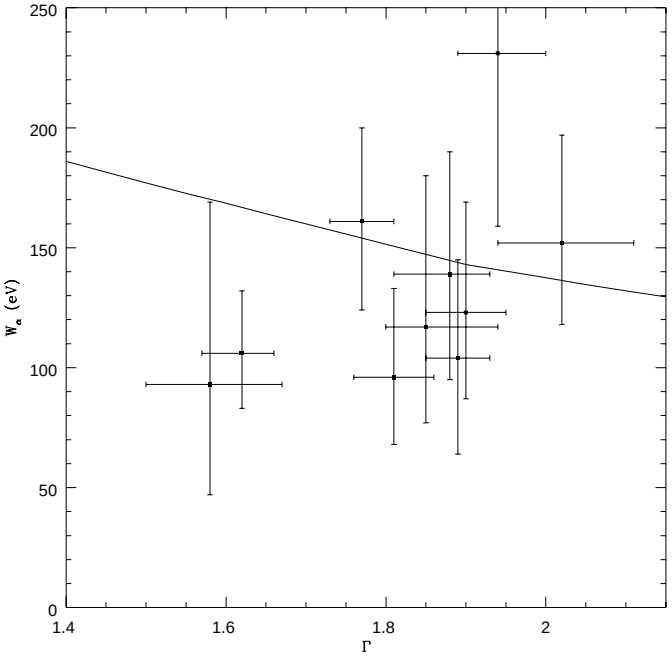

Fig. 3. W_α plotted versus Γ. The line, arbitrarily normalized, describes the trend expected (derived from George & Fabian 1991).

In addition to the one due to differences in the orientation, a scatter due to differences in abundance is expected in a graph of W_α versus Γ. A weak anticorrelation is predicted, with W_α decreasing with increasing Γ, as mentioned above. The line (arbitrary normalization) describing this effect (deduced from George & Fabian 1991) is plotted in the graph of W_α versus Γ in Fig. 3. Notably W_α shows instead a weak tendency to increase, on average, with Γ, which resembles that obtained by Lubiński & Zdziarski (2001, their Fig. 1). This is reflected in the sign of $r_\mathrm{s} = 0.57$, which, contrary to the prediction, is positive. The significance level for r_s deviating from zero is however 0.08, three times larger than in the previous case. We note, though, that in the fits the variable W_α is less dependent on Γ than the variable R: the same exercise performed for R, and just mentioned, yields differences in W_α which are at most, and typically less than 35% of their 90% confidence interval. Thus we are inclined to regard the evidence of a shallow trend in W_α increasing *on average* with Γ, albeit very marginal, no more so than it appears to be for R.

4.3. E_f versus Γ

The plot of E_f versus Γ in Fig. 4 appears to confirm the existence of a correlation, with E_f increasing on average with Γ, noted first in BeppoSAX data by Piro (1999) and then by Petrucci et al. (2001, their Fig. 6). Although the variable E_f in the fits, very much like R, is rather strongly dependent on Γ, and therefore one should not disregard the possibility that our result might be biased by this effect, we note that in this case the correlation coefficient r_s is equal to 0.88, and the significance level for r_s deviating from zero is comfortably lower and equal to 0.0007.

Discussing this correlation in terms of the mechanisms that give rise to the main spectral component goes beyond the scope of this paper (but see Petrucci et al. 2001). Our purpose here is to point out that, so long as one adopts the empirical representation of the direct continuum as a power law with an exponential cut–off, the existence of this type of correlation could, if ignored, artificially contribute to a correlation between R and Γ: in fact, as *Ginga* data do not allow to evaluate E_f, by either neglecting the exponential cut–off or keeping it at a fixed value irrespective of Γ (Zdziarski et al. 1999 choose $E_\mathrm{f} = 400$ keV fixed), one would systematically obtain lower values of R for lower values of Γ, for the reason already mentioned in Sect. 1. As an example of the interplay between E_f and R, we show the case of NGC 3783, whose Γ has an intermediate value in our sample: after excluding the cut–off we obtain $\chi^2 = 212.1/149$ ($\Delta\chi^2 = 61.7$ demonstrates the high significance of the cut–off in the fit given in Table 2) and a best fit value of $R = 0.38$ as opposed to $R = 0.63$. Although the effect is sizeable, it alone is probably insufficient to explain the difference in steepness of the correlation found in the *Ginga* sample by Zdziarski et al. (1999) and in our sample, but it does represent an explanation of the offset between *Ginga* and BeppoSAX results noted, and tentatively attributed to calibration differences, by the same authors.

5. Discussion and conclusions

In confronting theory of reprocessing in AGN and observations, first comes a test of the predicted correlation between the strength of the reflection and that of the iron line fluorescence relative to the primary photons in the

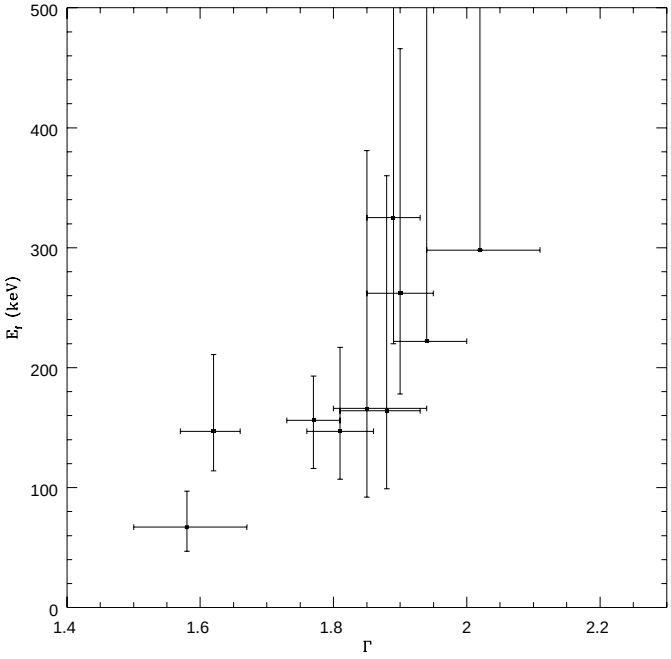

Fig. 4. The cut–off energy $E_{\rm f}$ plotted versus Γ.

PL, from material mainly at low ionization, as indicated by the observed energy of the line. Our test, while improving on it, does confirm the result originally obtained by Nandra & Pounds (1994), who compared the mean sample values of R and W_α with expectations from a face–on slab. We take properly into account the dependence of W_α on Γ in each observation and show that, be R intrinsically equal to one or otherwise, the amount of fluorescence is close to what expected from the strength of the reflection, and that a modest variance in the iron abundance is likely present. In doing that, we assume that the fairly substantial "narrow" contribution to the line, which from *Chandra* and XMM-*Newton* observations appears to be a rather common feature in this type of AGN, is associated with optically thick gas. This assumption needs to be checked in the future, at present, to our knowledge, it is observationally confirmed in only one of the objects in our sample, NGC 5506.

We have then tested the existence of a correlation in R and in W_α with respect to Γ. In both cases we find a marginal evidence of a very gradual increase, on average, with increasing spectral slope. The trend in W_α is qualitatively similar to that found in the larger sample of ASCA observations (Gaussian line fit) by Lubiński & Zdziarski (2001, their Fig. 1), while the one that we find in R is much shallower than that found by Zdziarski et al. (1999) in *Ginga* data. Partly this discrepancy could be due to the existence of a correlation, of which we have found evidence in our sample, between the e–folding energy $E_{\rm f}$ (spanning from about 80 keV to more than 300 keV) and Γ, which we took automatically into account in our fits, while Zdziarski et al. (1999) adopted a constant value equal to 400 keV. Thus our assessment, based on an admittedly much smaller sample of objects, is that the same phenomenological description of the spectral components, which are relevant to this issue, does not confirm the existence of a strong correlation between the relative strength of the Compton reflection, and the slope of the power law, while it provides some evidence that a very gradual correlation, and only on the average, for this quantity as well as for the iron line equivalent width, cannot be altogether excluded, but need to be confirmed with a sample of objects much larger than could be studied with BeppoSAX.

We conclude by commenting on three further limitations of this work. The first has to do with the narrow component of the line. On this matter further observational steps, which could not be pursued with BeppoSAX alone, are required, to disentangle the broad (accretion disk) component from the "narrow" component of the line, and simultaneously the fraction of the reflection associated with either of them. As recently shown by Malzac & Petrucci (2002) the nearly constant contribution by distant and thick matter, combined with a power law spectrum pivoting, as it varies in intensity, around energies in the range 1 to 10 keV, can introduce correlations between the reprocessing parameters and Γ. Their attempt to explain in this scenario the paradoxical result obtained on NGC 5548 by Chiang et al. (2000), mentioned in Sect. 3, is particularly suggestive.

The second limitation concerns the ionization structure and radiative transfer properties of the reprocessing material. Possibly with the exception of a fraction of line emission in NGC 5506 and Mrk 509, in our sample the adoption of a single zone, low ionization structure of the reflector seems fully justified. However, Done & Nayakshin (2001) have developed a disk model with a sharp transition from outer regions of low ionization to inner regions with a thick skin, highly or fully ionized, where the reflected continuum would be hard to distinguish from the direct continuum. In this model obviously the reflected fraction pertaining to the outer regions would present a value of R substantially less than unity. Moreover, their simulations of this model with the *Ginga* response, when fitted with the same model used by us, show that both R and W_α turn out to correlate with Γ in a rather gentle manner, qualitatively similar to our results. It would be interesting to see this exercise repeated with the wider band BeppoSAX response.

The third limitation has to do with the shape of the spectrum of the primary component. The conventional exponential factor adopted is useful to reproduce the steepening of the PL at high energies, as required by the data, but clearly the value of R which obtains is very sensitive to this shape. When using instead models of the continuum based on anisotropic comptonization in a disk corona (Haardt & Maraschi 1991; Haardt 1993) in fitting a sample of BeppoSAX observations, Petrucci et al. (2001) have shown that the value of R turns out different, typically larger than that provided by a description like the one used by us.

Thus on the whole there is still a very ample margin of progress to be made, before the confrontation between

theory and observations could be accomplished in a more satisfactory way.

Acknowledgements. The BeppoSAX satellite is a joint Italian–Dutch program. We are grateful to the BeppoSAX Scientific Data Centre (now ASI–SDC) for assistance. GCP thanks Fabio La Franca for help on a problem in statistics. This work was partially supported by the Italian Space Agency (ASI), and by the Ministry for University and Research (MIUR) under grant COFIN–00–02–36. POP acknowledges a grant of the European Commission under contract ERBFMRX-CT98-0195.

References

Anders, E., & Grevesse, N. 1993, Geochim. Cosmochim. Acta, 53, 197
Antonucci, R. 1993, ARA&A, 31, 473
Arnaud, K. A. 1996, in Astronomical Data Analysis Software and Systems V, ed. G. H. Jacoby, & J. Barnes (Astron. Soc. Pac., San Francisco), ASP Conf. Ser., 101, 17
Boella, G., Butler, R. C., Perola, G. C., et al. 1997a, A&AS, 122, 299
Boella, G., Chiappetti, L., Conti, G., et al. 1997b, A&AS, 122, 327
Chiang, J., Reynolds, C. S., Blaes, O. M., et al. 2000, ApJ, 528, 292
Costantini, E., Nicastro, F., Fruscione, A., et al. 2000, ApJ, 544, 283
De Rosa, A., Piro, L., Fiore, F., et al. 2002, A&A, 387, 838
Done, C., Madejski, G. M., & Życki, P. T. 2000, ApJ, 536, 213
Done, C., & Nayakshin, S. 2001, ApJ, 546, 419
Elvis, M., Lockman, F. J., & Wilkes, B. 1989, AJ, 97, 777
Fabian, A. C., Rees, M. J., Stella, L., & White, N. E. 1989, MNRAS, 238, 729
Fabian, A. C., Iwasawa, K., Reynolds, C. S., & Young, A. J. 2000, PASP, 112, 1145
Fiore, F., Guainazzi, M., & Grandi, P. 1999, SDC report (available from `http://www.asdc.asi.it/bepposax/software/index.html`)
Frontera, F., Costa, E., Dal Fiume, D., et al. 1997, A&AS, 122, 357
George, I. M., & Fabian, A. C. 1991, MNRAS, 249, 352
George, I. M., Turner, T. J., Netzer, H., et al. 1998, ApJS, 114, 73
Ghisellini, G., Haardt, F., & Matt, G. 1994, MNRAS, 267, 743
Gilli, R., Maiolino, R., Marconi, A., et al. 2000, A&A, 355, 485
Gondoin, P., Barr, P., Lumb, D., et al. 2001, A&A, 378, 806
Guainazzi, M., Nicastro, F., Fiore, F., et al. 1998, MNRAS, 301, L1
Guainazzi, M., Perola, G. C., Matt, G., et al. 1999a, A&A, 346, 407
Guainazzi, M., Matt, G., Molendi, S., et al. 1999b, A&A, 341, L27
Guainazzi, M., Marshall, W., & Parmar, A. N. 2001, MNRAS, 323, 75
Guilbert, P. W., & Rees, M. J. 1988, MNRAS, 233, 475
Haardt, F., & Maraschi, L. 1991, ApJ, 380, L51
Haardt, F. 1993, ApJ, 413, 680
Jourdain, E., Bassani, L., Buchet, L., et al. 1992, A&A, 256, L38
Kaastra, J. S., & Barr, P. 1989, A&A, 226, 59
Kaastra, J. S., Steenbrugge, K. C., Raassen, A. J. J., et al. 2002, A&A, 386, 427
Kaspi, S., Brandt, W. N., Netzer, H., et al. 2001, ApJ, 554, 216
Lamer, G., Uttley, P., & McHardy, I. M. 2000, MNRAS, 319, 949
Lampton, M., Margon, B., & Bowyer, S. 1976, ApJ, 208, 177
Lightman, A. P., & White, T. R. 1988, ApJ, 335, 57
Lubiński, P., & Zdziarski, A. A. 2001, MNRAS, 323, L37
Magdziarz, P., & Zdziarski, A. A. 1995, MNRAS, 273, 837
Magdziarz, P., Blaes, O. M., Zdziarski, A. A., Johnson, W. N., & Smith, D. A. 1998, MNRAS, 301, 179
Malzac, J., & Petrucci, P.-O. 2002, MNRAS, submitted
Matsuoka, M., Piro, L., Yamauchi, M., & Murakami, T. 1990, ApJ, 361, 440
Matt, G., Perola, G. C., & Piro, L. 1991, A&A, 247, 25
Matt, G., Fabian, A. C., & Reynolds, C. S. 1997, MNRAS, 289, 175
Matt, G., Guainazzi, M., Perola, G. C., et al. 2001, A&A, 377, L31
Murphy, E. M., Lockman, F. J., Laor, A., & Elvis, M. 1996, ApJS, 105, 369
Nandra, K., & Pounds, K. A. 1994, MNRAS, 268, 405
Nandra, K., George, I. M., Mushotzky, R. F., Turner, T. J., & Yaqoob, T. 1997, ApJ, 477, 602
Nandra, K., Le, T., George, I. M., et al. 2000, ApJ, 544, 734
Nicastro, F., Piro, L., De Rosa, A., et al. 2000, ApJ, 536, 718
Parmar, A. N., Martin, D. D. E., Bavdaz, M., et al. 1997, A&AS, 122, 309
Perola, G. C., Matt, G., Cappi, M., et al. 1999, A&A, 351, 937
Perola, G. C., Matt, G., Fiore, F., et al. 2000, A&A, 358, 117
Petrucci, P. O., Haardt, F., Maraschi, L., et al. 2001, ApJ, 556, 716
Piro, L., Yamauchi, M., & Matsuoka, M. 1990, ApJ, 360, L35
Piro, L. 1999, Astron. Nachr., 320, 236
Piro, L., Nicastro, F., Perola, G. C., et al. 2001, ApJ, submitted
Pounds, K. A., Nandra, K., Stewart, G. C., George, I. M., & Fabian, A. C. 1990, Nature, 344, 132
Pounds, K., Reeves, J., O'Brien, P., et al. 2001, ApJ, 559, 181
Press, W. H., Flannery, B. P., Teukolsky, S. A., & Vetterling, W. T. 1992, Numerical Recipes (Cambridge Univ. Press, Cambridge)
Smith, D. A., & Done, C. 1996, MNRAS, 280, 355
Tanaka, Y., Nandra, K., Fabian, A. C., et al. 1995, Nature, 375, 659
Vaughan, S., & Edelson, R. 2001, ApJ, 548, 694
Véron-Cetty, M. P., & Véron, P. 1993, ESO Scientific Report, 13
Weaver, K. A., Yaqoob, T., Mushotzky, R. F., et al. 1997, ApJ, 474, 675
Weaver, K. A., Krolik, J. H., & Pier, E. A. 1998, ApJ, 498, 213
Weaver, K. A., Gelbord, J., & Yaqoob, T. 2001, ApJ, 550, 261
Weaver, K. A. 2001, in The central kpc of starbursts and AGN: the La Palma connection, ed. J. H. Knapen, J. E. Beckman, I. Shlosman, & T. J. Mahoney, ASP Conf. Ser., in press [`astro-ph/0108481`]
Woźniak, P. R., Zdziarski, A. A., Smith, D., Madejski, G. M., & Johnson, W. N. 1998, MNRAS, 299, 449
Yaqoob, T., George, I. M., Nandra, K., et al. 2001, ApJ, 546, 759
Yaqoob, T., Padmanabhan, U., Dotani, T., & Nandra, K. 2002, ApJ, 569, 487
Zdziarski, A. A., Lubiński, P., & Smith, D. A. 1999, MNRAS, 303, L11